Future Engineering Journal

Volume 3 | Issue 1 Article 4

November 2021

Structural Dynamics of AWT-27 Wind Turbine Blade

Amr Ismaiel
Future University in Egypt (FUE), amr.mohamed@fue.edu.eg

FUTURE ENGINEERING JOURNAL 3 (2022) 2314-7237

Future Engineering Journal

Journal homepage: http://digitalcommons.aaru.edu.jo/fej/

Structural Dynamics of AWT-27 Wind Turbine Blade

Amr Ismaiel [a,*]

[a] *Mechanical Engineering Department, Future University in Egypt (FUE), Cairo, Egypt.*

ARTICLEINFO

Article history:

Received April 2022
Received in revised form April 2022
Accepted May 2022

Keywords:

Wind Turbine
AWT-27
Structure Dynamics
Turbulence

ABSTRACT

Wind energy is one of the world's current leading renewable energy resources. One of the major aspects of studying wind turbines is the structural dynamics for the turbine structure including blades and support structure. In the current work, the blades of the Advanced Wind Turbine (AWT-27) are investigated in a dynamic approach. Different wind fields have been generated for the study to provide different Design Load Conditions (DLCs). Three laminar wind velocities of 5 m/s, 12 m/s, and 17 m/s were simulated. Turbulent wind flow fields have also been generated at the three standard classes A, B and C of high, medium, and low turbulence intensities respectively. The generated wind fields are used as inputs to calculate the aerodynamic loads for each wind condition using the Blade Element Momentum (BEM) theory. Aerodynamic loads have been calculated, namely, the shear force on five different locations along the blade length. Results of the simulation are summarized such that the shear forces at the blade root, 30%, 50%, 70% of the blade length are known for each wind condition. The summary serves as a guide for further optimization of the blade structural design.

1. Introduction

Wind energy is one of the world's fastest-growing sources of renewable energy. Each year, new installations of wind power are achieved worldwide. By the end of the year 2020, the global cumulative installed wind power has reached 743 GW (GWEC 2021). With the high demand for energy and the lack of energy sources, researchers from all over the world compete to improve the harvesting of wind power.

New trends and techniques have been innovated to harvest wind power in different methods. Those methods include using airborne vehicles to generate energy using the wind. Examples of airborne wind energy (AWE) are the kite wind power systems (Dief, et al. 2018) (Rushdi, et al. 2020), tethered wing power systems (Kakavand and Nikoobin 2021), and airborne vehicles (Makani n.d.). Some other trends also include bladeless wind turbines (Adeyanju and Boucher 2020) (Francis, Umesh, and Shivakumar 2021). However, wind turbines are still the most common and most installed wind power systems. Research studies conducted on wind turbines are concerned with improving the behavior of wind turbines from aerodynamic, structural, and control points of view.

The structural dynamics of a wind turbine's blade and tower play a major role in the lifetime of a wind turbine which is typically 20 years of operation (Ismaiel, Metwalli, et al. 2017). The stochastic nature of wind induces severe dynamic loads on the wind turbine's blades and tower. Turbulence in wind has been proven to affect the fatigue life of a wind turbine negatively, hence, the study of dynamic wind loads is crucial to the structural design of a wind turbine (Ismaiel and Yoshida 2018).

Different approaches have been adopted to study wind turbines' blades and towers structure dynamics. These approaches include analytical methods where the blades can be simplified to a cantilever and then, Euler beam theory can be used for the analysis (Nagulesawaran 2004). This approach was also used in an aeroelastic analysis where the coupling between aerodynamic loads and inertial loads resulting from the blades vibrations is considered (Ismaiel and Yoshida 2019) (Ismaiel and Yoshida 2020). Another analytical approach is the transfer matrix method, which was used and compared to finite element analysis for the study of structure dynamics (Fayzollahzadeh, et al. 2016). Numerical methods were also useful to perform structural analysis studies, Finite

* *Corresponding author.* At Mechanical Engineering Department, Future University in Egypt Tel.: +20-103-3100-227
E-mail address: *amr.mohamed@fue.edu.eg*

Peer review under responsibility of Faculty of Engineering and Technology, Future University in Egypt.

https://digitalcommons.aaru.edu.jo/fej/

Element Models (FEM) were utilized for many different dynamic loading conditions including wind variations, tower shadow effect (Murtagh, Basu and Broderick 2005), and earthquake excitations (Kiyomiya, Rikiji and Gelder 2002). Despite the high accuracy of the finite element approach, the main drawback is the high computational cost.

In this work, the blades of National Renewable Energy Laboratory's (NREL) two-bladed Advanced Wind Turbine 26/27 (AWT-27) are analyzed dynamically. A numerical approach using deterministic models is used to calculate the aerodynamic loads on the blades of the turbine for different laminar and turbulent wind conditions. This work aims to provide a guide for structural design optimization for the blades of the AWT-27 wind turbine. Different Design Load Conditions (DLCs) are presented and the aerodynamic loads are calculated and provided for further improvement of the blades structure based on these loads.

2. Basic Models and Methodology

In this section, the basic wind turbine model and the methodology followed will be introduced. The AWT-27 wind turbine will be defined, then the generation of wind fields will be explained. Finally, the methodology for the aerodynamic load calculations will be mentioned.

2.1. AWT-27 Wind Turbine Definition

Advanced Wind Turbine (AWT-27) was first developed after a cooperation between the National Renewable Energy Laboratory (NREL) and R. Lynette & Associates corporation in the year 1990 (Poore 1998). The AWT-27 is a utility-grade downwind two-bladed wind turbine which comes in different configurations with different capacities. Downwind wind turbines are in an orientation where the rotor comes downwind of the tower in the wind direction. Although the tower effect becomes more effective for downwind wind turbines, the blades can be designed to be more flexible and hence less weight. Figure 1 shows the orientation of a two-bladed downwind turbine.

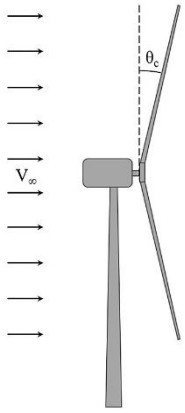

Fig. 1. Orientation of a Two-bladed Downwind Wind Turbine (Noyes, Qin and Loth 2018)

As mentioned before, the turbine is designed for different capacities. The configuration chosen for study in this work is the AWT-27 configuration with a capacity of 275 kW. The turbine is a horizontal axis with a blade length of 13.5 m and rotor diameter of 28.5 m. Table 1 shows the main features of the AWT-27 wind turbine.

Table 1. Main Features of AWT-27 Wind Turbine (Poore 1998)

Property	**Status/Value**
Orientation	Downwind
Number of blades	2
Blade length (m)	13.5
Rotor diameter (m)	28.5
Hub height (m)	42.6
Cone angle (deg)	7
Tilt angle (deg)	0
Cut-in wind speed (m/s)	4.9
Rated wind speed (m/s)	17
Cut-out wind speed (m/s)	22.5
Rated power (kW)	275
Airfoil type (Root, Midspan, and Tip)	NLF 422, NLF 418, and NLF 416
Chord (mm) (Root, Max, and Tip)	500, 1200, and 368
Blade material	Fiberglass Epoxy

2.2. Wind Field Generation

In order to study different loading conditions, different wind fields should be generated before calculating the aerodynamic loads on the blade. The software TurbSim has been used for generation of wind fields (Jonkman and Kilcher 2012). The software generates laminar and turbulent flow fields, and takes into account the turbine geometry such that the wind field covers the total area of the rotor at the hub height.

Five different wind conditions were generated for further aerodynamic loads calculations. Three laminar wind fields at wind velocities right after cut-in wind speed with a value of 5 m/s, intermediate speed of 12 m/s, and rated wind speed of 17 m/s. Furthermore, two turbulent fields at average wind speeds of 5 m/s and 12 m/s. Each wind speed is simulated at three different turbulence intensities of classes A (High turbulence), B (Medium turbulence), and C (Low turbulence) according to the International Electrotechnical Commission (IEC) standards for wind turbines (IEC 2005).

Turbulence intensity can be defined as the standard deviation of wind speeds divided by the mean value of wind speeds over a certain amount of time. TurbSim software generates turbulent fields using spectral models with depends on the frequency and then a time series of wind velocities can be obtained. Among the spectral models used in TurbSim is the Kaimal model which was adopted in this study since it gives a better description of atmospheric turbulence than other spectral models. The Kaimal model can be explained in Equation 1.

$$\frac{nS_u(n)}{\sigma_u^2} = \frac{4nL_{1u}/\overline{U}}{(1+6nL_{1u}/\overline{U})^{5/3}} \qquad \text{Eq. (1)}$$

Where n is the frequency, $S_u(n)$ is the wind's spectral density function, σ_u is the wind speed's standard deviation in the longitudinal direction, L_{1u} is a length scale with values depending on the surface roughness and the above ground height, and $\overline{U}$ is the mean wind speed. Figures 2 and 3 show the generated turbulent fields for wind speeds of 5 m/s and 12 m/s respectively.

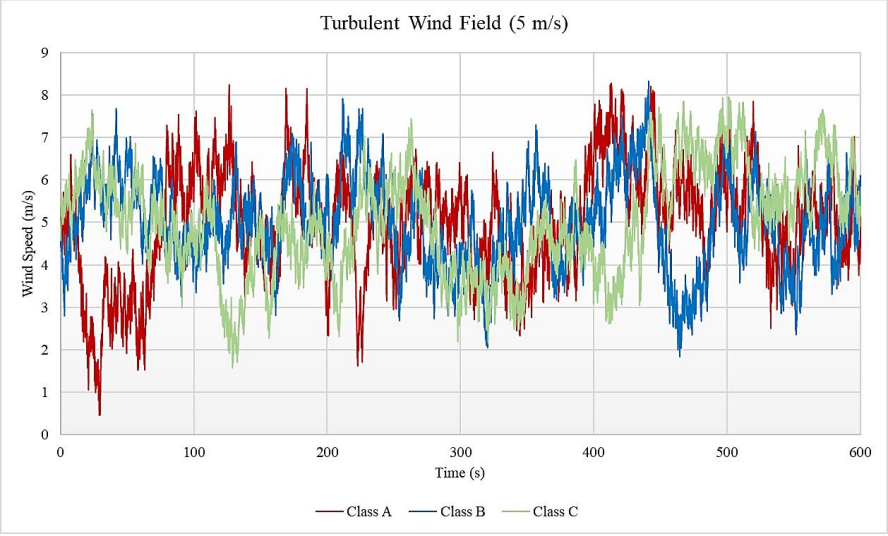

Fig. 2. Turbulent Wind Field for Average Wind Speed of 5 m/s (Turbulence Classes A, B, and C)

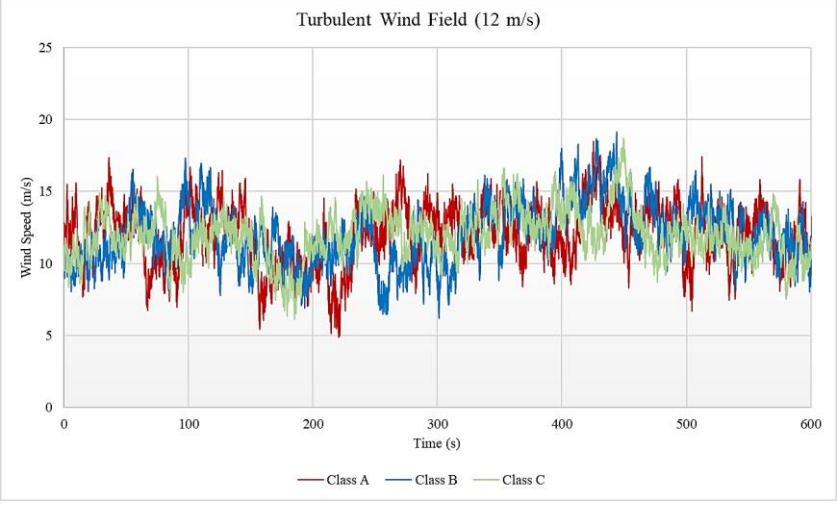

Fig. 3. Turbulent Wind Field for Average Wind Speed of 12 m/s (Turbulence Classes A, B, and C)

2.3. Aerodynamic Loads Calculation

The software used for calculating the aerodynamic loads is NREL's aeroelastic tool FAST (Jonkman and Buhl 2005). FAST is a multi-body aeroelastic tool that utilizes different modules for aerodynamics, elastic structures, and baseline control, together with wind conditions and other operating conditions. The basic theory used in FAST for the aerodynamic loads' calculation is the Blade Element Momentum (BEM) theory. BEM couples both the momentum theory and the blade element theory, and then determines the loads in the flaps (Out-of-rotor-plane), and edgewise (In-plane) loads. The rotor is divided into annular elements along the blade length, then the lift (L) and drag (D) forces are calculated at each element, and finally, the loads normal (P_N) and tangent (P_T) to the rotor plane can be found using Equations 2 and 3. Figure 4 shows the cross-section of the blade with different loads on it.

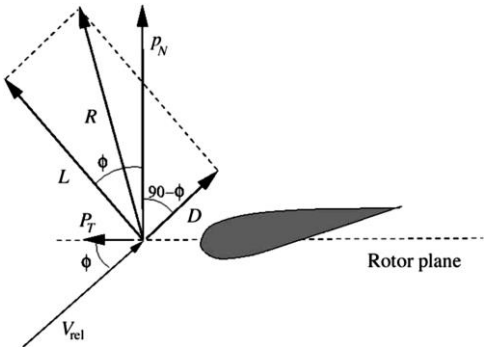

Fig. 4. Loads on the Cross-Section of the Blade (Hansen 2008)

$$P_N = L\cos\varphi + D\sin\varphi \qquad \text{Eq. (2)}$$

$$P_T = L\sin\varphi - D\cos\varphi \qquad \text{Eq. (3)}$$

Where φ is the flow angle at each cross-section.

The simulation is performed for the aforementioned wind conditions, and the loads on the blades were calculated over time in a dynamic behavior.

3. Results and Discussion

In this section, results of the FAST simulation will be shown. As mentioned before, wind fields was generated for laminar and turbulent conditions. Results of the laminar wind field will be shown, then the turbulent wind conditions. The shear forces in the flaps and edgewise directions are calculated at five different locations along the blade length, namely at the blade root, at 30%, 50%, 70% of the blade length, and at the blade root.

3.1. Laminar Wind Fields

Simulations are performed for three different laminar wind speeds. First speed is 5 m/s, which is right after the turbine's cut-in wind speed of 4.9 m/s. Figures 5-9 show the shear forces in the flaps (Out-of-plane) and edgewise (In-plane) directions at the selected locations on the blade.

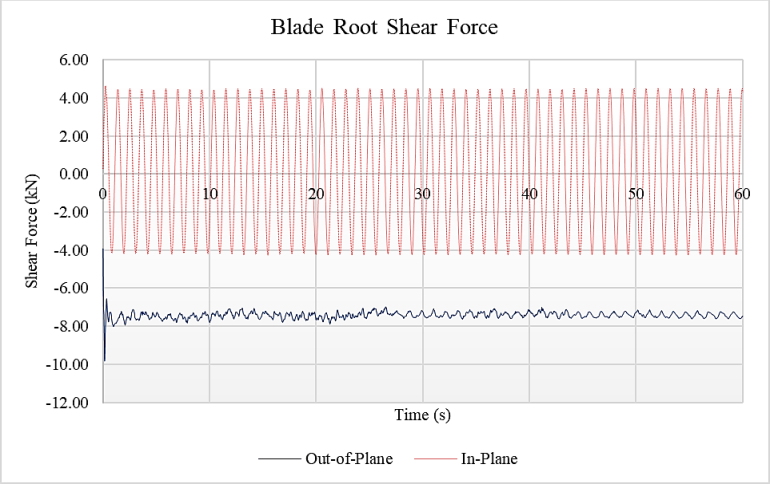

Fig. 5. Shear Force at the Blade Root (Wind Speed = 5 m/s)

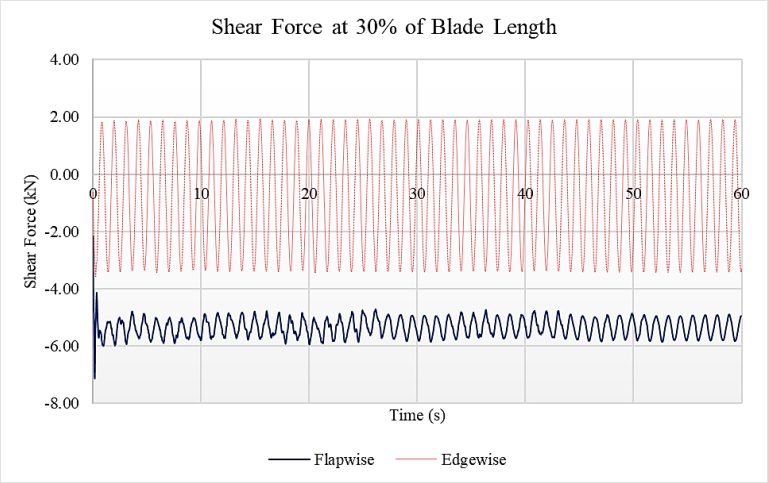

Fig. 6. Shear Force at 30% of the Blade Length (Wind Speed = 5 m/s)

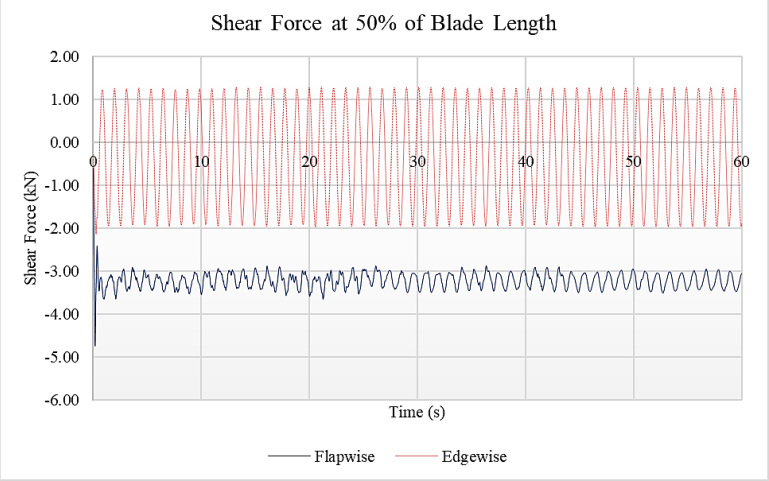

Fig. 7. Shear Force at 50% of the Blade Length (Wind Speed = 5 m/s)

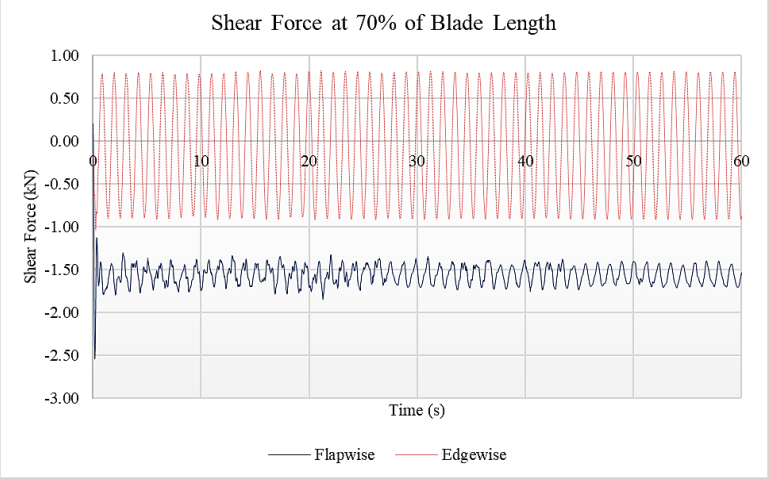

Fig. 8. Shear Force at 70% of the Blade Length (Wind Speed = 5 m/s)

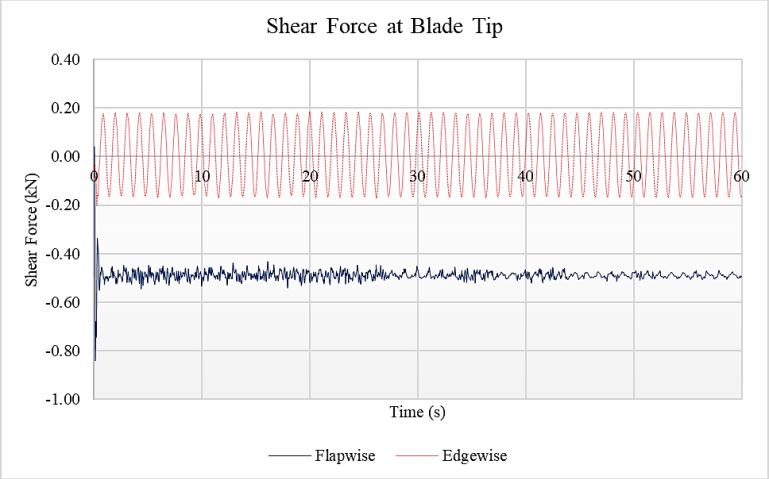

Fig. 9. Shear Force at the Blade Tip (Wind Speed = 5 m/s)

For the laminar wind case, the simulation was performed for 60 seconds since the loads settle after few seconds, and there is no big change in the range of values and the loads have nearly sinusoidal behaviour. The sinusoidal behaviour of the loads come from the fact that the blades when rotate in the rotor plane, the gravity plays a major role in the inertial loads, specially that the blades are not in an upright position with the presence of a coning angle of 7°.

Bending moments are also crucial for the structural design of a turbine's blade. The bending moment is maximum at the blade's root, and can be found by integrating the shear forces on the blade. Bending moment at the blade root is shown in Figure 10.

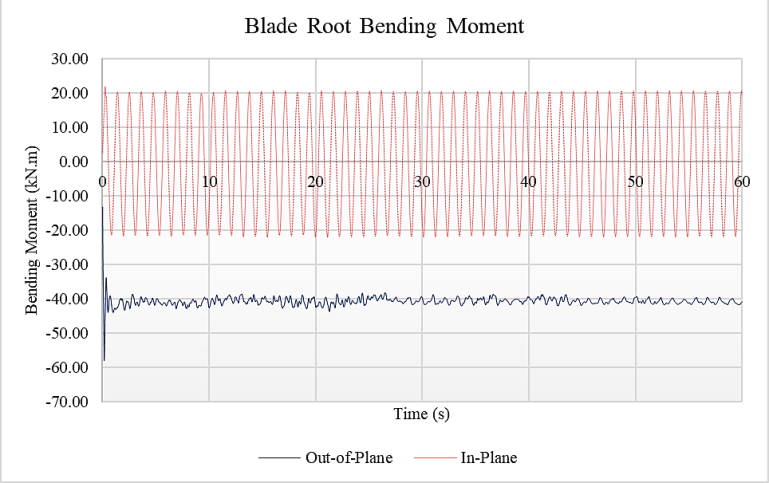

Fig. 10. Bending Moment at the Blade Root (Wind Speed = 5 m/s)

The aerodynamic loads are observed to be of a sinusoidal behaviour with a very high frequency. Even though the flow is laminar with no turbulence, the dynamic loads still exist. As mentioned earlier, this behaviour is due to the inertial loads resulting from the blade's azimuth position in the rotor plane. Because of this dynamic nature of aerodynamic loads, it is very important to study the effect of the loads on the fatigue lifetime of the turbine to avoid failure. Structure dynamics should be studied for the design of a wind turbine blade or tower.

The original turbine's blade is made of Fiberglass reinforced with epoxy. The basic structural properties, stiffness and mass distributions of the original blade can be found in the definition report (Poore 1998). Based on the original blade, an aeroelastic simulation has been performed as well to calculate the deflections of the blade. The most critical point for deflection is at the blade tip. Figure 11 shows the blade tip deflections for the first condition of laminar wind speed of 5 m/s.

The same simulations have been performed for the other two laminar wind fields. However, the results will only be summarized by their mean values and standard deviations later on.

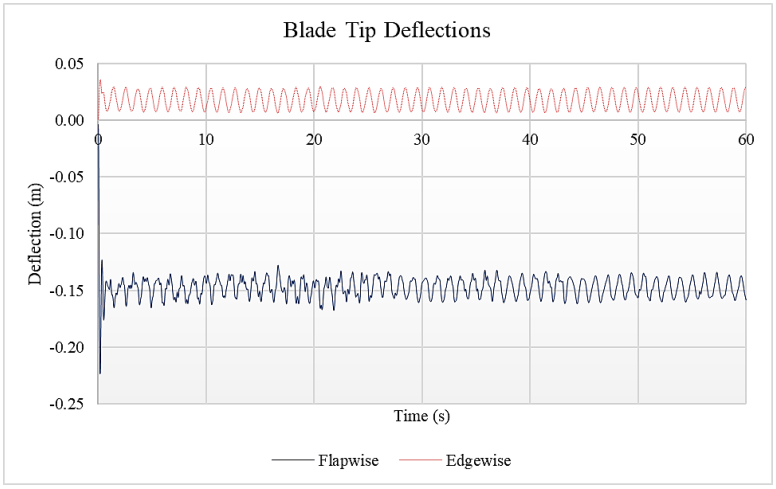

Fig. 11. Deflections at the Blade Tip (Wind Speed = 5 m/s)

3.2. Turbulent Wind Fields

Similarly, the simulations have been performed for the turbulent flow fields. For an average wind speed of 5 m/s, three turbulent fields with high turbulence intensity (Class A), medium intensity (Class B), and low intensity (Class C) were generated. The same turbulence classes were also used for an average wind speed of 12 m/s. In this section, results for turbulence flow field with an average wind speed of 5 m/s and turbulence class A will be shown.

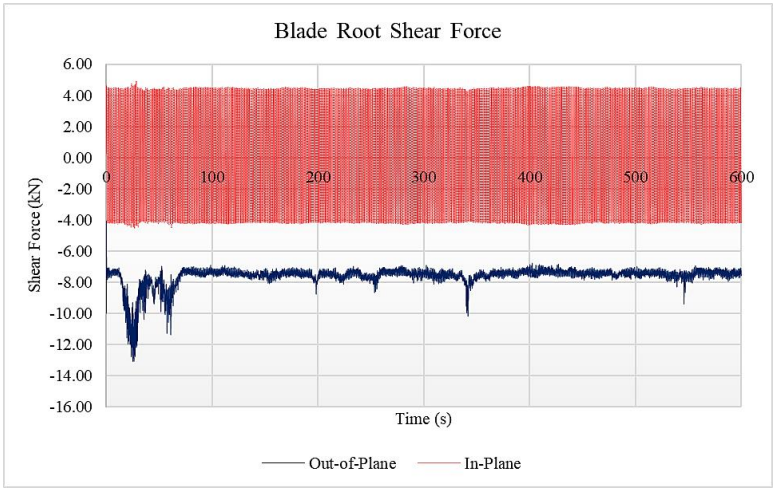

Fig. 12. Shear Force at the Blade Root (Turb. Class A, Average Wind Speed = 5 m/s)

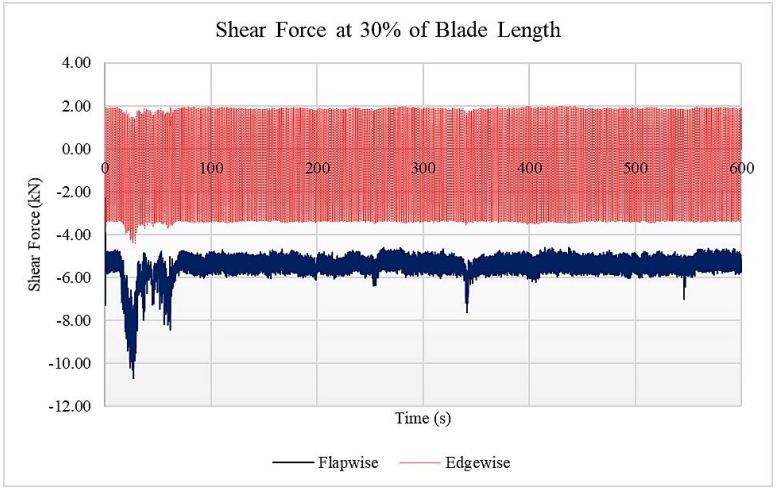

Fig. 13. Shear Force at 30% of the Blade Length (Turb. Class A, Average Wind Speed = 5 m/s)

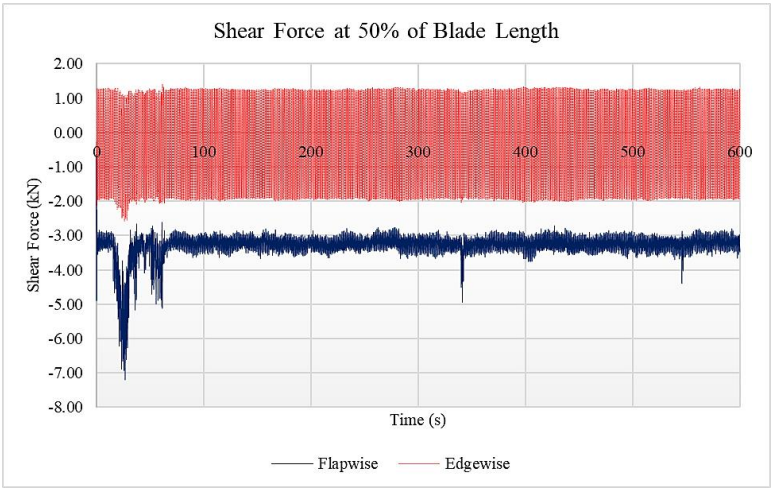

Fig. 14. Shear Force at 50% of the Blade Length (Turb. Class A, Average Wind Speed = 5 m/s)

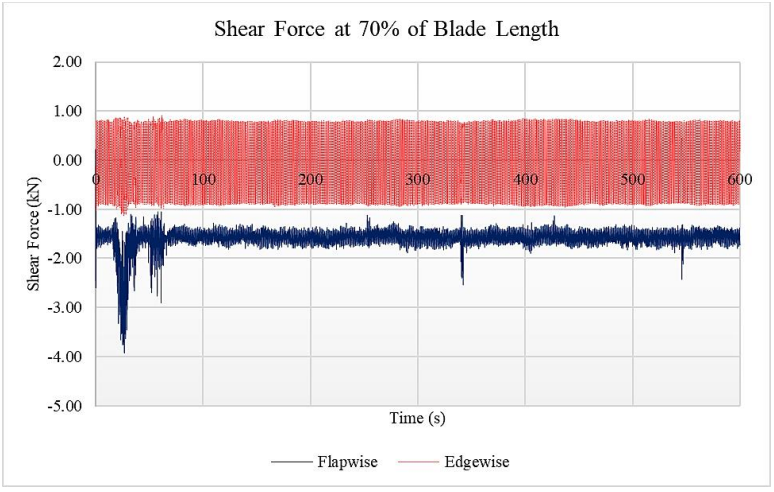

Fig. 15. Shear Force at 70% of the Blade Length (Turb. Class A, Average Wind Speed = 5 m/s)

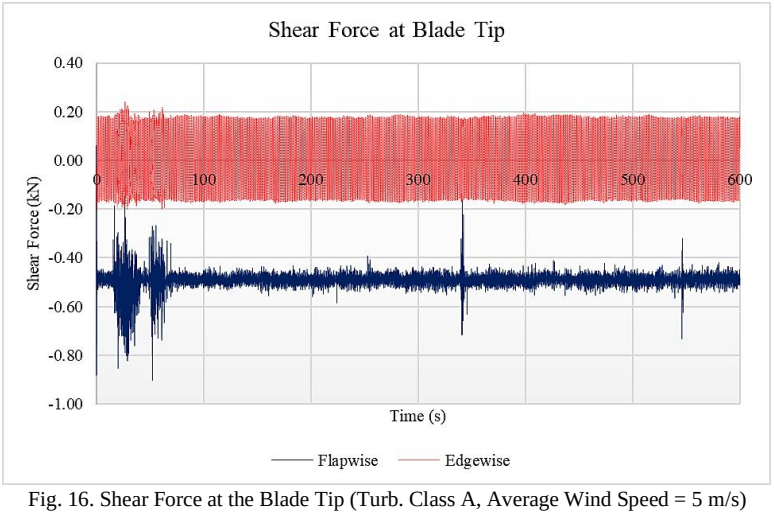

Fig. 16. Shear Force at the Blade Tip (Turb. Class A, Average Wind Speed = 5 m/s)

For the turbulent flow field, it is a common practice to run the simulation for a physical time of 10 minutes. The turbulent behaviour is highly nonlinear, and compared to laminar flow field, 60 seconds are not enough to judge the turbulent behaviour. Hence, all the turbulent simulations where run for 600 s.

As shown in the figures, the turbulence has resulted in a more severe dynamic behaviour of the aerodynamic loads over the blades. Not only the range of values has increased compared to the laminar flow case, but also the frequency of change has increased drastically. Another observation is that the load does not settle at a certain value over time, excitations in the wind field can lead to excitation in the dynamic loads. Not to mention the danger of resonance if the frequency of the wind coincides with the natural frequencies of the blade. For this reason, modal analysis should also be performed during the design of a wind turbine blade. Usually, the first and second modes of vibration in the flapwise direction, and the first mode in the edgewise direction are the most important modes for structural design. Higher modes of vibration can be neglected.

Similar to the laminar flow condition, the bending moment at the blade root can be calculated by integrating the shear forces along the blade. Figure 17 shows the blade root bending moment.

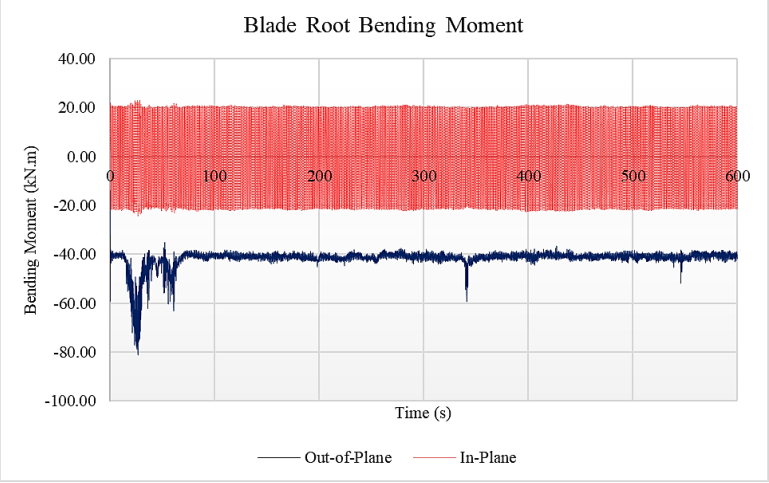

Fig. 17. Bending Moment at the Blade Root (Turb. Class A, Average Wind Speed = 5 m/s)

Deflections at the blade tip were calculated for the original turbine blade, results are shown in Figure 18.

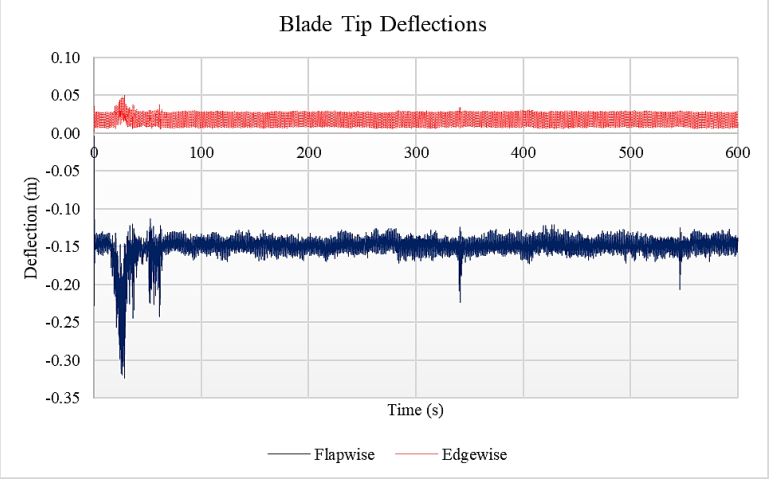

Fig. 18. Deflections at the Blade Tip (Turb. Class A, Average Wind Speed = 5 m/s)

It can be observed that the major difference between the laminar flow field and turbulent flow field is in the frequency by which the loads change their values. The higher the turbulence intensity, the higher the frequency of aerodynamic loads.

The results of the remaining wind fields will be shown in terms of statistical values instead of charts. The results for all wind fields are summarized in Table 2.

Table 2. Summary of Shear Forces for All Wind Conditions

Laminar Flow – Wind Speed = 5 m/s										
Quantity	**Flapwise Shear Force (kN)**					**Edgewise Shear Force (kN)**				
Location on Blade	**Root**	**30%**	**50%**	**70%**	**Tip**	**Root**	**30%**	**50%**	**70%**	**Tip**
Minimum	-9.827	-7.136	-4.745	-2.539	-0.838	-4.251	-3.594	-2.133	-1.036	-0.203
Maximum	-3.922	-2.154	-0.596	0.204	0.041	4.638	1.934	1.291	0.821	0.184
Mean	-7.414	-5.340	-3.218	-1.558	-0.488	0.148	-0.760	-0.344	-0.052	0.006
Standard Deviation	0.188	0.320	0.186	0.120	0.024	3.071	1.871	1.132	0.601	0.121
Laminar Flow – Wind Speed = 12 m/s										
Quantity	**Flapwise Shear Force (kN)**					**Edgewise Shear Force (kN)**				
Location on Blade	**Root**	**30%**	**50%**	**70%**	**Tip**	**Root**	**30%**	**50%**	**70%**	**Tip**
Minimum	-9.671	-7.631	-5.061	-2.756	-0.666	-4.57	-3.789	-2.207	-1.028	-0.207
Maximum	-2.901	-1.461	-0.149	0.368	-0.228	4.77	2.213	1.45	0.891	0.209
Mean	-6.292	-4.427	-2.596	-1.233	-0.475	0.066	-0.683	-0.312	-0.059	0.004
Standard Deviation	1.210	1.052	0.770	0.467	0.059	3.038	1.845	1.112	0.588	0.119
Laminar Flow – Wind Speed = 17 m/s										
Quantity	**Flapwise Shear Force (kN)**					**Edgewise Shear Force (kN)**				
Location on Blade	**Root**	**30%**	**50%**	**70%**	**Tip**	**Root**	**30%**	**50%**	**70%**	**Tip**
Minimum	-10.56	-7.843	-5.029	-2.751	-0.728	-5.008	-3.906	-2.301	-1.088	-0.226
Maximum	-1.32	-0.034	0.666	0.752	-0.099	4.906	2.477	1.613	0.953	0.229
Mean	-5.693	-3.928	-2.231	-1.019	-0.460	-0.014	-0.665	-0.308	-0.071	0.002
Standard Deviation	1.802	1.535	1.127	0.682	0.088	3.034	1.842	1.109	0.585	0.118
Turbulent Flow – *Class A*, Average Wind Speed = 5 m/s										
Quantity	**Flapwise Shear Force (kN)**					**Edgewise Shear Force (kN)**				
Location on Blade	**Root**	**30%**	**50%**	**70%**	**Tip**	**Root**	**30%**	**50%**	**70%**	**Tip**
Minimum	-13.1	-10.7	-7.2	-3.93	-0.904	-4.56	-4.42	-2.59	-1.14	-0.204
Maximum	-4.07	-2.26	-0.634	0.218	0.061	4.92	1.99	1.4	0.919	0.241
Mean	-7.612	-5.468	-3.283	-1.587	-0.491	0.126	-0.774	-0.347	-0.051	0.006
Standard Deviation	0.604	0.554	0.352	0.197	0.030	3.067	1.86	1.131	0.601	0.121
Turbulent Flow – *Class B*, Average Wind Speed = 5 m/s										
Quantity	**Flapwise Shear Force (kN)**					**Edgewise Shear Force (kN)**				
Location on Blade	**Root**	**30%**	**50%**	**70%**	**Tip**	**Root**	**30%**	**50%**	**70%**	**Tip**
Minimum	-10.12	-8.046	-4.892	-2.894	-0.860	-4.378	-3.609	-2.097	-1.016	-0.198
Maximum	-4.01	-2.132	-0.592	0.160	0.015	4.637	2.026	1.368	0.885	0.207
Mean	-7.531	-5.40	-3.235	-1.567	-0.490	0.127	-0.761	-0.340	-0.049	0.006
Standard Deviation	0.304	0.351	0.183	0.116	0.022	3.064	1.866	1.129	0.599	0.121
Turbulent Flow – *Class C*, Average Wind Speed = 5 m/s										
Quantity	**Flapwise Shear Force (kN)**					**Edgewise Shear Force (kN)**				
Location on Blade	**Root**	**30%**	**50%**	**70%**	**Tip**	**Root**	**30%**	**50%**	**70%**	**Tip**
Minimum	-9.819	-7.123	-4.726	-2.526	-0.884	-4.319	-3.595	-2.129	-1.035	-0.203
Maximum	-3.986	-2.149	-0.642	0.156	0.037	4.656	1.972	1.333	0.869	0.206
Mean	-7.531	-5.396	-3.230	-1.566	-0.489	0.127	-0.760	-0.339	-0.049	0.0067
Standard Deviation	0.251	0.323	0.168	0.105	0.016	3.064	1.866	1.128	0.599	0.121
Turbulent Flow – *Class A*, Average Wind Speed = 12 m/s										
Quantity	**Flapwise Shear Force (kN)**					**Edgewise Shear Force (kN)**				
Location on Blade	**Root**	**30%**	**50%**	**70%**	**Tip**	**Root**	**30%**	**50%**	**70%**	**Tip**
Minimum	-15.16	-11.81	-8.143	-4.688	-0.96	-5.12	-4.418	-2.622	-1.201	-0.238
Maximum	-1.049	0.217	0.779	0.755	0.156	5.238	2.426	1.621	1.021	0.248
Mean	-7.945	-5.809	-3.609	-1.829	-0.515	0.086	-0.867	-0.414	-0.077	0.0055
Standard Deviation	2.184	1.850	1.360	0.818	0.099	3.079	1.895	1.149	0.609	0.124

Turbulent Flow – *Class B*, Average Wind Speed = 12 m/s										
Quantity	**Flapwise Shear Force (kN)**					**Edgewise Shear Force (kN)**				
Location on Blade	**Root**	**30%**	**50%**	**70%**	**Tip**	**Root**	**30%**	**50%**	**70%**	**Tip**
Minimum	-14.57	-11.52	-7.831	-4.46	-1.205	-4.892	-4.368	-2.636	-1.208	-0.232
Maximum	-0.836	0.769	0.972	0.819	0.268	4.883	2.4	1.599	0.979	0.225
Mean	-7.923	-5.791	-3.594	-1.819	-0.515	0.0838	-0.861	-0.409	-0.075	0.0057
Standard Deviation	2.125	1.791	1.303	0.772	0.0871	3.074	1.886	1.143	0.606	0.123
Turbulent Flow – *Class C*, Average Wind Speed = 12 m/s										
Quantity	**Flapwise Shear Force (kN)**					**Edgewise Shear Force (kN)**				
Location on Blade	**Root**	**30%**	**50%**	**70%**	**Tip**	**Root**	**30%**	**50%**	**70%**	**Tip**
Minimum	-15.3	-11.69	-8.067	-4.84	-1.007	-4.99	-4.544	-2.755	-1.288	-0.222
Maximum	-0.935	0.104	0.769	0.718	0.109	4.89	2.354	1.543	0.960	0.223
Mean	-7.926	-5.794	-3.597	-1.823	-0.515	0.102	-0.846	-0.400	-0.070	0.006
Standard Deviation	1.810	1.528	1.107	0.658	0.076	3.074	1.884	1.141	0.605	0.122

The results in Table 2 can be further used for fatigue analysis of the blade. It can be also used for optimization of the blade structural design such that the blade deflections are reduced, and failure is avoided.

4. Conclusions

In this work, the blade of an AWT-27 wind turbine is analyzed dynamically. Aerodynamic loads calculations have been performed for different Design Load Conditions (DLCs). The wind field has been generated for three different laminar wind velocities of 5 m/s, 12 m/s, and 17 m/s. Turbulence wind field has also been simulated for the three IEC standard turbulence intensities of classes A, B, and C for high, medium, and low turbulence respectively. The generated wind fields have been used as an input to calculate the aerodynamic loads using the Blade Element Momentum theory through FAST software.

Shear forces in the flaps (Out-of-plane) and edgewise (In-plane) directions at 5 different locations along the blade. The locations are at the blade root, at 30%, 50%, 70% of the blade length, and at the blade tip. Results have shown that there is a dynamic behavior of the loads even for the laminar wind condition due to the inertial loads at different azimuth positions of the blade. For the turbulent flow field, not only the values of shear forces have increased, but also the frequency of the dynamic loads increase.

The severe dynamic nature of the aerodynamic loads leads to severe fatigue loading and hence affects the fatigue lifetime of the turbine blade negatively. A thorough dynamic structure analysis should be followed to account for the high-frequency dynamics at different wind conditions. Results of the shear loads over the blade have been summarized for the different investigated wind conditions. This summary serves as a guide for further optimizing the blade structural design based on different loading conditions to reduce the blade deflections and stresses.

REFERENCES

Adeyanju, A. A., and D. Boucher. 2020. "Theoretical Analysis of the Bladeless Wind Turbine Performance." *Journal of Scientific Research and Reports* 26 (10): 93-106. doi:10.9734/jsrr/2020/v26i1030325.

Dief, Tarek, Uwe Fechner, Roland Schmehl, Shigeo Yoshida, Amr Ismaiel, and Amr M. Halawa. 2018. "System identification, fuzzy control and simulation of a kite power system with fixed tether length." *Wind Energy Science* (3): 275-291. doi:10.5194/wes-3-275-2018.

Fayzollahzadeh, M., M. J. Mahmoodi, S. M. Yadavar-Nikravesh, and J. Jamali. 2016. "Wind load response of offshore wind turbine towers with fixed monopile platform." *Journal of Wind Engineering and Industrial Aerodynamics* 158: 122-128.

Francis, S., V. Umesh, and S. Shivakumar. 2021. "Design and Analysis of Vortex Bladeless Wind Turbine." *Materials Today: Proceedings* 47 (11): 5584-5588. doi:10.1016/j.matpr.2021.03.469.

GWEC. 2021. *Global Wind Report.* Brussels: Global Wind Energy Council.

Hansen, M. O. L. 2008. "Steady BEM Model." In *Aerodynamics of Wind Turbines*. London: Earthscan.

IEC. 2005. "Wind turbines – Part 1: Design requirements, International Standard 61400–1 (3rd edition)." Standard.

Ismaiel, Amr, and Shigeo Yoshida. 2020. "Aeroelastic Analysis for Side-Booms of a Coplanar Twin-Rotor Wind Turbine." *International Review of Aerospace Engineering* 13 (4): 135-140. doi:10.15866/irease.v13i4.18355.

Ismaiel, Amr, and Shigeo Yoshida. 2019. "Aeroelastic Analysis of a Coplanar Twin-Rotor Wind Turbine." *Energies* 12 (10): 1881. doi:10.3390/en12101881.

Ismaiel, Amr, and Shigeo Yoshida. 2018. "Study of turbulence intensity effect on the fatigue lifetime of wind turbines." *Evergreen* 5 (1): 25-32. doi:10.5109/1929727.

Ismaiel, Amr, Sayed M Metwalli, Basman Elhadidi, and Shigeo Yoshida. 2017. "Fatigue Analysis of an Optimized HAWT Composite Blade." *Evergreen* 4 (2/3): 1-6. doi:10.5109/1929656.

Jonkman, B. J., and L. Kilcher. 2012. *TurbSim User's Guide.* Technical Report, Golden, Colorado: NREL.

Jonkman, Jason, and Marshall Buhl. 2005. *FAST User's Guide.* User Guide, Golden, Colorado: NREL.

Kakavand, M., and A. Nikoobin. 2021. "Numerical simulation of tethered-wing power systems based on variational integration." *Journal of Computational*

Science 51 (2): 101351. doi:10.1016/j.jocs.2021.101351.

Kiyomiya, O., T. Rikiji, and P. H. van Gelder. 2002. "Dynamic response analysis of onshore wind energy power units during earthquakes and wind." *The 12th International Offshore and Polar Engineering Conference.* OnePetro.

Makani. n.d. *Makani.* Accessed 3 18, 2022. https://x.company/projects/makani/.

Murtagh, P. J., B. Basu, and B.M. Broderick. 2005. "Along-wind response of a wind turbine tower with blade coupling subjected to rotatationally sampled wind loading." *Engineering Structures* 27 (8): 1209-1219.

Nagulesawaran, S. 2004. "Lateral vibration of a centrifucgally tensioned uniform Euler-Bernoulli beam." *Journal of sound and vibration* 176 (5): 613-624.

Noyes, Carlos, Chao Qin, and Eric Loth. 2018. "Pre-aligned downwind rotor for a 13.2 MW wind turbine." *Renewable Energy* 116: 749-754. doi:10.1016/j.renene.2017.10.019.

Poore, R. 1998. *NWTC AWT-26 Research and Retrofit Project Summary of AWT-26/27 Turbine Research and Development.* Golden - Colorado: NREL.

Rushdi, M. A., A. Rushdi, T. Dief, A. M. Halawa, S. Yoshida, and R. Schmehl. 2020. "Power Prediction of Airborne Wind Energy Systems Using Multivariate Machine Learning." *Energies* 13 (9): 2367. doi:10.3390/en13092367.